AGU PUBLICATIONS

Global Biogeochemical Cycles

RESEARCH ARTICLE

10.1002/2014GB004933

Key Points:
- The modeled Southern Ocean carbon sink has weakened during the observed period
- Long-term trends in pCO_2 can be used as a proxy for changes in the CO_2 sink
- It is not yet possible to detect a weakening of the sink from pCO_2 observations

Correspondence to:
N. S. Lovenduski,
nicole.lovenduski@colorado.edu

Citation:
Lovenduski, N. S., A. R. Fay, and G. A. McKinley (2015), Observing multidecadal trends in Southern Ocean CO_2 uptake: What can we learn from an ocean model?, *Global Biogeochem. Cycles*, *29*, 416–426, doi:10.1002/2014GB004933.

Received 9 JUL 2014
Accepted 8 MAR 2015
Accepted article online 11 MAR 2015
Published online 10 APR 2015

Observing multidecadal trends in Southern Ocean CO_2 uptake: What can we learn from an ocean model?

Nicole S. Lovenduski[1], Amanda R. Fay[2], and Galen A. McKinley[3]

[1]Department of Atmospheric and Oceanic Sciences and Institute of Arctic and Alpine Research, University of Colorado Boulder, Boulder, Colorado, USA, [2]Space Science and Engineering Center, University of Wisconsin, Madison, Wisconsin, USA, [3]Department of Atmospheric and Oceanic Sciences, University of Wisconsin, Madison, Wisconsin, USA

Abstract We use output from a hindcast simulation (1958–2007) of an ocean biogeochemical and ecological model to inform an observational strategy for detection of a weakening Southern Ocean CO_2 sink from surface ocean pCO_2 data. Particular emphasis is placed on resolving disparate conclusions about the Southern Ocean CO_2 sink that have been drawn from surface ocean pCO_2 observation studies in the past. We find that long-term trends in $\Delta pCO_2 (pCO_2^{oc} - pCO_2^{atm})$ can be used as a proxy for changes in the strength of the CO_2 sink but must be interpreted with caution, as they are calculated from small differences in the oceanic and atmospheric pCO_2 trends. Large interannual, decadal, and multidecadal variability in ΔpCO_2 persists throughout the simulation, suggesting that one must consider a range of start and end years for trend analysis before drawing conclusions about changes in the CO_2 sink. Winter-mean CO_2 flux trends are statistically indistinguishable from annual-mean trends, arguing for inclusion of all available pCO_2^{oc} data in future analyses of the CO_2 sink. The weakening of the CO_2 sink emerges during the observed period of our simulation (1981–2007) in the subpolar seasonally stratified biome (4°C < average climatological temperature < 9°C); the weakening is most evident during periods with positive trends in the Southern Annular Mode. With perfect temporal and spatial coverage, 13 years of pCO_2^{oc} data would be required to detect a weakening CO_2 sink in this biome. Given available data, it is not yet possible to detect a weakening of the Southern Ocean CO_2 sink with much certainty, due to imperfect data coverage and high variability in Southern Ocean surface pCO_2.

1. Introduction

The growth rate of atmospheric carbon dioxide (CO_2) has increased over the past several decades [*Canadell et al.*, 2007]. Some studies suggest that the increase in growth rate is due in part to a decline in the efficiency of the oceanic sink for atmospheric CO_2 [*Le Quéré et al.*, 2010; *Le Quéré*, 2010], though the uncertainties in the magnitude of this decline are quite large [*McKinley et al.*, 2011; *Fay and McKinley*, 2013]. Given the important role of atmospheric CO_2 in the climate system, and the ocean's strong influence on atmospheric CO_2, there is a critical need to accurately monitor changes in the oceanic sink for atmospheric CO_2.

The Southern Ocean is a major sink of atmospheric CO_2, contributing to over 40% of the current inventory of anthropogenic CO_2 in the ocean [*Khatiwala et al.*, 2009]. Several recent model studies suggest that the Southern Ocean CO_2 sink has saturated over the past few decades. The saturation of the CO_2 sink is caused by a poleward intensification of the Southern Hemisphere westerly winds. In these models, the wind trend drives an increase in the meridional overturning and upwelling of carbon-rich waters to the surface, where the excess carbon remains unconsumed by biology and escapes to the atmosphere, thus reducing the efficacy of the Southern Ocean CO_2 sink [*Le Quéré et al.*, 2007; *Lovenduski et al.*, 2008; *Lovenduski and Ito*, 2009].

Model-estimated changes of the saturating Southern Ocean CO_2 sink and the mechanisms driving this saturating sink need to be validated with observations. Coarse-resolution models with parameterized eddies may not accurately represent the Southern Ocean meridional overturning response to poleward-intensified wind stress [*Gent and Danabasoglu*, 2011] and therefore the advection of natural dissolved inorganic carbon that is critical to determining the Southern Ocean CO_2 sink efficacy [*Lovenduski et al.*, 2013]. A recent study based on observations of CFC-12 finds that Southern Ocean meridional overturning has increased from the early 1990s to the late 2000s [*Waugh et al.*, 2013], confirming the mechanism described in coarse-resolution modeling studies. Models also have wildly inaccurate representations of chlorophyll concentration in the

Southern Ocean [*Strutton et al.*, 2012], calling into question model-estimated changes in biological production under poleward-intensified wind [*Wang and Moore*, 2012]. Observational studies find a wide range of trends in Southern Ocean net community production over the past few decades [*Munro et al.*, 2015].

Ultimately, determining whether the Southern Ocean CO_2 sink has saturated and by how much over the past several decades requires direct observation of changes in the Southern Ocean sea-air CO_2 fluxes. As direct observations of sea-air CO_2 flux are rare in the Southern Ocean, recent studies have compared changes in observed oceanic pCO_2 with changes in atmospheric pCO_2 over the same period to infer whether the Southern Ocean CO_2 sink has changed with time [*Metzl*, 2009; *Takahashi et al.*, 2009, 2012; *Lenton et al.*, 2012; *Fay and McKinley*, 2013]. In these studies, if oceanic pCO_2 has risen faster than atmospheric pCO_2 over a given period, it is often inferred that the CO_2 sink has weakened in this period. However, the Southern Ocean exhibits high interannual and decadal variability in air-sea CO_2 flux that must be considered when evaluating trends [*Wetzel et al.*, 2005; *Lovenduski et al.*, 2007; *Lenton and Matear*, 2007; *Verdy et al.*, 2007; *Lenton et al.*, 2013], and there is considerable disagreement in the literature about whether pCO_2 observations indicate a weakening Southern Ocean CO_2 sink over the past few decades.

A recent study of wintertime pCO_2 observations in the source region for Antarctic Intermediate Water finds that surface ocean pCO_2 has increased at a rate faster than the atmospheric increase rate during 1986 to 2010 and suggests that the CO_2 sink has weakened in this region [*Takahashi et al.*, 2012]. The analysis focuses on wintertime pCO_2 observations because biological activities are at a minimum and vertical mixing of carbon-rich deep waters is at a maximum in this season; it may therefore be possible to see a wintertime trend in vertical mixing or meridional overturning from the surface ocean pCO_2 data. The surface ocean pCO_2 data are binned according to local sea surface temperature and divided into five temperature zones between 0.8°C and 5.5°C. The middle three temperature zones (1.5°C–4.5°C) exhibit a surface ocean pCO_2 trend of 24.4 ± 3.3 μatm decade^{-1}, significantly above the atmospheric pCO_2 trend of 16 μatm decade^{-1}, indicating a weakening of the CO_2 sink in this region of the Southern Ocean.

In contrast, a study of year-round pCO_2 observations in the Southern Ocean using the Takahashi LDEO database finds that for a range of start and end years from 1981 to 2010, trends in surface ocean pCO_2 are largely statistically indistinguishable from trends in atmospheric pCO_2, indicating that the Southern Ocean CO_2 sink is unchanging over this period [*Fay and McKinley*, 2013]. The analysis uses all of the available surface ocean pCO_2 data, regardless of season or location, but corrects for spatial bias by removing a background pCO_2 climatology from all observations before fitting harmonic trends. The surface ocean pCO_2 data are binned over physical biomes; in the Southern Ocean two biomes are analyzed: the marginal sea ice biome (average climatological temperature < 4°C) and the subpolar seasonally stratified biome (4°C < average climatological temperature < 9°C). Trends in surface ocean pCO_2 are compared to trends in atmospheric pCO_2 for a range of start and end years in each biome. In both biomes, the trends in the surface ocean pCO_2 are largely similar to the trends in atmospheric pCO_2, indicating an unchanging CO_2 sink in these regions of the Southern Ocean.

The disparate conclusions about the changing Southern Ocean CO_2 sink drawn from recent pCO_2 observational studies invite further investigation into data analysis techniques and raise broad questions about the data that can be addressed with ocean models. A companion paper [*Fay et al.*, 2014] studies the impacts that methodological choices can have on the analysis of Southern Ocean pCO_2 trends, focusing on region definitions, time series selection, and spatial biasing of data. Here, we use output from a hindcast simulation (1958–2007) of an ocean biogeochemical and ecological model to address questions about the utility of surface ocean pCO_2 data in estimating multidecadal trends in the Southern Ocean CO_2 sink. Throughout the manuscript, we aim to answer the following questions:

1. Do trends in $\Delta pCO_2 (pCO_2^{oc} - pCO_2^{atm})$ indicate trends in sea-air CO_2 flux in the Southern Ocean, or do trends in the gas exchange coefficient (via trends in wind) and solubility (via trends in temperature) compromise the signal?
2. Are Southern Ocean CO_2 flux trends affected by the choice of start/end year or seasonal period of analysis (wintertime vs. year-round)?
3. Where are the Southern Ocean CO_2 flux trends most robust?
4. Do we have enough surface ocean pCO_2 data to detect a weakening of the Southern Ocean CO_2 sink?

We begin in section 2 with a description of our model and statistical analysis techniques and then show our main results in section 3. In section 4, we conclude our study by answering these questions and discussing their implications for observation of the changing Southern Ocean CO_2 sink.

2. Methods

2.1. Model Description

We analyze output from a hindcast simulation of the Community Earth System Model (CESM) ocean physical component with embedded biogeochemistry and ecology [*Lovenduski et al.*, 2013]. The physical model is the ocean component of the Community Climate System Model version 4 [*Danabasoglu et al.*, 2012]. The model has nominal 1° horizontal resolution and 60 vertical levels. Mesoscale eddy transport is parameterized with an updated version of *Gent and McWilliams* [1990], where the eddy-induced advection coefficient, κ, is diagnosed as a function of space and time. Diapycnal mixing is represented using the K-Profile Parameterization of *Large et al.* [1994], and mixed layer restratification by submesoscale eddies is parameterized using the method of *Fox-Kemper et al.* [2011]. The biogeochemical-ecosystem model consists of an upper ocean ecological module which incorporates multinutrient co-limitation on phytoplankton growth and specific phytoplankton functional groups [*Moore et al.*, 2004], and a full-depth ocean biogeochemistry module which incorporates full carbonate system thermodynamics, sea-air CO_2 fluxes, and a dynamic iron cycle [*Doney et al.*, 2006; *Moore and Braucher*, 2008].

In the hindcast configuration, the ocean and sea ice components of CESM are forced with atmospheric observations and reanalyses from 1948 to 2007, following the Coordinated Ocean-ice Reference Experiments protocol [*Griffies et al.*, 2009; *Large and Yeager*, 2009]. The initial physical state was taken from a previous ocean-ice hindcast simulation, and biogeochemical fields were initialized with the observationally-based climatology of *Key et al.* [2004]. Four repeating 60 year forcing cycles were conducted with full ocean biogeochemistry, and the physical fields were reset to their initial conditions at the beginning of each cycle. Here, we analyze the final 50 years of the hindcast simulation (1958-2007), omitting the first 10 years after the abrupt restart of the forcing. Two simulations are analyzed: in the first, atmospheric CO_2 is held at 284.7 ppm, and in the second, the time-varying historical record of atmospheric CO_2 is used as a surface boundary condition [*Long et al.*, 2013]. The sea-air CO_2 fluxes from the first simulation are that of natural carbon, the second simulation produces contemporary CO_2 fluxes, and the anthropogenic CO_2 fluxes can be estimated by subtraction [*Lovenduski et al.*, 2007].

The model successfully reproduces sea surface temperature distributions and Drake Passage transport [*Danabasoglu et al.*, 2012] and captures the broad spatiotemporal patterns in air-sea CO_2 fluxes [*Long et al.*, 2013]. For the final 10 years of the simulation, the spatially integrated sea-air flux of CO_2 for the Southern Ocean is -0.37 Pg C yr^{-1}, the sum of a natural flux of 0.22 Pg C yr^{-1} and an anthropogenic flux of -0.59 Pg C yr^{-1}. Multidecadal trends in the advection, mixing, and sea-air flux of natural CO_2 in the Southern Ocean were previously investigated using output from this hindcast simulation in *Lovenduski et al.* [2013]. The model predicts an increase in the sea-air flux of natural CO_2 over the 50 year simulation, caused by wind-driven increases in the advection and diapycnal mixing of natural dissolved inorganic carbon (DIC).

2.2. Statistical Analysis

All trends described in this paper represent the slope of a line which exhibits the best fit to the model output in a least-squares sense. We report trends over the full model simulation (*simulated period*; 1958 to 2007), for the period in which we have sufficient observations of surface ocean pCO_2 (*observed period*; 1981 to 2007), and for a range of start and end years, as in *McKinley et al.* [2011] and *Fay and McKinley* [2013]. We separately consider trends in annual-mean model output and trends in wintertime average (July to November, as in *Takahashi et al.* [2012]) model output. Significance of trends is calculated as by *Santer et al.* [2000], while accounting for autocorrelation in the time series [*Bretherton et al.*, 1999].

The length of time series, n^*, required to detect a trend of given magnitude, ω_0, at the 90% confidence level is calculated as in *Weatherhead et al.* [1998]:

$$n^* = \left[\frac{3.3\sigma_N}{|\omega_0|}\sqrt{\frac{1+\phi}{1-\phi}}\right]^{2/3}, \quad (1)$$

where σ_N and ϕ are the standard deviation and autocorrelation, respectively, of the residuals after the trend has been removed. This statistical technique was applied successfully to satellite chlorophyll data in *Henson*

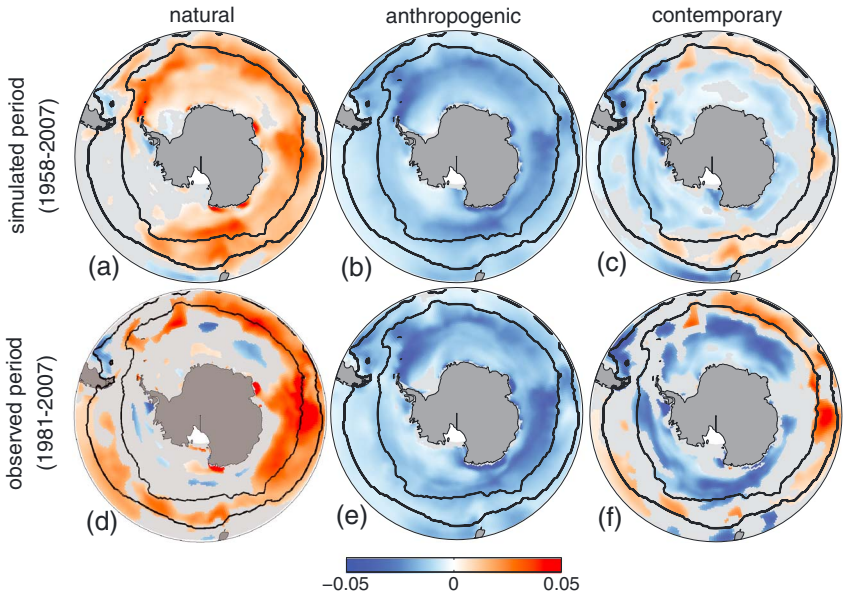

Figure 1. Model-estimated trends in the sea-air flux of (first column) natural, (second column) anthropogenic, and (third column) contemporary CO_2 over (first row) the simulated period (1958–2007) and (second row) the observed period (1981–2007). Units are mol C m^{-2} yr^{-2}, and positive indicates CO_2 outgassing trend. Only those trends with significance ≥ 95% are shown. Black lines mark the edges of the model biomes used the study. From south to north, these biomes are the Southern Ocean seasonally ice covered biome (SO-ICE) and the Southern Ocean subpolar seasonally stratified biome (SO-SPSS).

et al. [2010]; it provides a way to quantify the importance of the variance and autocorrelation of the data on the detection of the trend.

We estimate trends by binning the Southern Ocean model output into two biogeographical biomes: the marginal sea ice biome (SO-ICE; annual-mean temperature < 4°C) and the subpolar seasonally stratified biome (SO-SPSS; 4°C < annual-mean temperature < 9°C), as in *Fay and McKinley* [2013]. This method uses modeled surface temperature to create static geographic boundaries for statistical analysis.

3. Results and Discussion

Previous modeling studies have noted that the saturation of the Southern Ocean CO_2 sink over the past few decades is driven by a trend toward anomalous outgassing of natural CO_2 from the Southern Ocean, while anthropogenic CO_2 has exhibited an ingassing trend over the same period [e.g., *Lovenduski et al.*, 2008]. In Figure 1, we investigate these trends separately for the simulated period and the observed period. Throughout the Southern Ocean, we find a positive trend in the outgassing of natural CO_2 (Figures 1a and 1d). The spatial pattern and magnitude of the trend is sensitive to the period being analyzed: the trend is more widespread over the simulated period, but larger, particularly in the SO-SPSS region, during the observed period. Anthropogenic CO_2 exhibits negative trends over both periods, with the largest trends in the SO-ICE region (Figures 1b and 1e).

The superposition of the trends in the natural and anthropogenic CO_2 fluxes creates a complex spatial pattern in the trends of the contemporary CO_2 flux that is sensitive to the period being analyzed (Figures 1c and 1f). Over both the simulated and observed periods, we find negative trends in the SO-ICE region and positive trends in the SO-SPSS region, but the magnitude of the trends is larger in the observed period. Therefore, it may be possible to detect a weakening of the Southern Ocean CO_2 sink (observationally this would be detected as a positive trend in the contemporary CO_2 flux) in the SO-SPSS region during the observed period.

We investigate whether quantification of trends in ΔpCO_2 (i.e., $pCO_2^{oc} - pCO_2^{atm}$) from observed data is sufficient to determine trends in the contemporary CO_2 flux in Figure 2. Here, the trends in average contemporary CO_2 flux over the SO-SPSS region are decomposed into contributions from trends in ΔpCO_2, piston velocity, and solubility using a linear Taylor expansion of annual-mean model output (see Appendix A

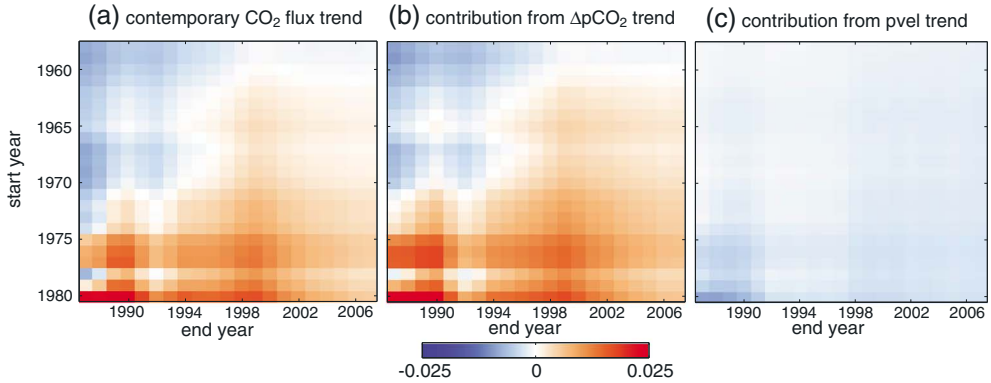

Figure 2. Trends in the SO-SPSS average (a) sea-air flux of contemporary CO_2 for a range of start and end years, and the contribution to the CO_2 flux trend from (b) the trend in ΔpCO_2 and (c) the trend in the piston velocity. Units are mol C m^{-2} yr^{-2}, and positive denotes CO_2 outgassing trend.

for more details; note that sea ice fraction is zero in SO-SPSS). CO_2 flux trends and their contributions are calculated for a range of start years (*y* axis; 1958–1980) and end years (*x* axis; 1986–2007) over the simulated period, capturing the evolution of the SO-SPSS contemporary CO_2 flux trends shown in Figures 1c and 1f. Here, positive numbers indicate a contribution toward a CO_2 outgassing trend, or a weakening of the CO_2 sink, during that period. During the early part of our simulation, the CO_2 sink in the SO-SPSS region is strengthening; a weakening of the CO_2 sink is not observed until the later part of the simulation (Figure 2a). The CO_2 flux trends are largely driven by trends in ΔpCO_2 (Figure 2b), while trends in the piston velocity contribute to small negative CO_2 flux trends for all periods (Figure 2c). The contribution from the trend in solubility is near zero for all periods (not shown). From this decomposition, we conclude that observation of trends in ΔpCO_2 is sufficient to determine trends in the contemporary CO_2 flux, as trends in piston velocity and solubility make only small contributions to the total CO_2 flux trend. Therefore, by measuring trends in ΔpCO_2, we may be able to observe a weakening of the Southern Ocean CO_2 sink.

The ΔpCO_2 trends are driven by subtle differences between the trends in pCO_2^{oc} and pCO_2^{atm}. Figure 3 shows that in the SO-SPSS region, both oceanic and atmospheric pCO_2 increase with time, due to the anthropogenic perturbation in atmospheric CO_2 and the uptake of that perturbation by the ocean. The atmospheric pCO_2 is, at all times, larger than the oceanic pCO_2, indicating that this region is typically a sink for atmospheric CO_2. For a range of start and end years, pCO_2^{oc} has only a slightly different slope from pCO_2^{atm}; it is this small difference that drives a change in the strength of the CO_2 sink in this region. Oceanic pCO_2 exhibits much more variability than atmospheric pCO_2. In Figure 3, oceanic pCO_2 variability is decomposed into two driving components: the component driven by changes in surface temperature (pCO_2-T) and the remaining variability due to biological and chemical factors (pCO_2-nonT; see Appendix B for more details). De-trended surface ocean pCO_2 anomalies have a strong, positive correlation with pCO_2-nonT anomalies ($r = 0.95$) and a weak, negative correlation with pCO_2-T anomalies ($r = -0.58$), and 70% of the trend in surface ocean pCO_2 can be explained by the trend in pCO_2-nonT. This decomposition suggests that biological and chemical factors, namely surface salinity, alkalinity, and dissolved inorganic carbon, drive both the variability and positive trend in SO-SPSS surface ocean pCO_2. This is consistent with *Lovenduski et al.* [2013], who show that dissolved inorganic carbon is the primary driver of the weakening CO_2 sink in this region. We note that while the pCO_2-T trend in SO-SPSS is negligible, this may not be the case in other regions (e.g., the North Atlantic), where surface warming is likely an important

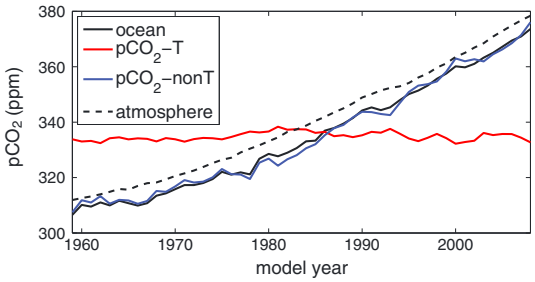

Figure 3. Average annual-mean surface ocean and atmospheric pCO_2 in the SO-SPSS region. Surface ocean pCO_2 is decomposed into the component due to temperature (pCO_2-T) and the remaining variability due to biological and chemical factors (pCO_2-nonT).

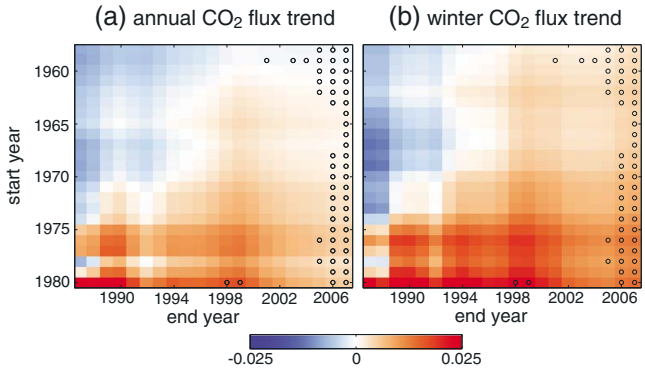

Figure 4. Trends in the SO-SPSS average sea-air flux of contemporary CO_2 for (a) annual-mean (same as Figure 2a) and (b) wintertime model output, for a range of start and end years. Units are mol C m^{-2} yr^{-2}, and positive denotes outgassing trend. Open black circles indicate time periods for which the annual-mean trends are statistically different from the wintertime trends.

component of the observed CO_2 flux changes [*Sarmiento and Le Quéré*, 1996; *Le Quéré et al.*, 2010; *McKinley et al.*, 2011; *Fay and McKinley*, 2013].

We compare SO-SPSS winter-mean and annual-mean CO_2 flux trends for a range of start and end years during the simulated period in Figure 4. Consistent with the annual-mean CO_2 fluxes, winter-mean fluxes show a strengthening of the CO_2 sink (negative flux trends) during the early part of the simulation and a weakening of the CO_2 sink (positive flux trends) during the later part of the simulation. We determine whether the difference between the winter-mean and annual-mean trends is statistically significant by estimating the 95% confidence interval for each annual-mean trend. If the winter-mean trend falls outside of this interval, we indicate this with an open circle in Figure 4. We conclude from this analysis that trends calculated with only wintertime observations are statistically indistinguishable from trends calculated using all available observations during the year for most start and end years, with the exception of end years 2006 and 2007, when the region is a strong source of CO_2 in the wintertime. This conclusion is supported by the pCO_2 observational data analysis presented in *Fay et al.* [2014]. Given the lack of available Southern Ocean pCO_2^{oc} observations in the wintertime relative to other seasons [*Takahashi et al.*, 2012], and the perfect temporal coverage afforded by the model, this analysis supports the inclusion of all available pCO_2^{oc} observations when investigating changes in the Southern Ocean CO_2 sink.

The trends in the modeled fluxes of contemporary CO_2 evolve differently in the two Southern Ocean biomes. In SO-ICE, the contemporary CO_2 flux trend is near zero in the early part of the simulation (1958–1980; constant CO_2 sink), and negative in the later part of the simulation (1981–2007; strengthening CO_2 sink; Figure 5a). In the early part of the simulation, the flux of natural CO_2 in SO-ICE exhibits a positive trend which is balanced by a negative trend in the flux of anthropogenic CO_2; in the later part of the simulation, the negative trend in the flux of anthropogenic CO_2 is larger than the trend toward natural CO_2 outgassing. In SO-SPSS, the contemporary CO_2 flux trend is negative during the early part of the simulation, when the negative trend in anthropogenic CO_2 flux exceeds the near-zero trend in natural CO_2 flux (Figure 5b). The weakening of the Southern Ocean CO_2 sink (positive trend in contemporary CO_2 flux) emerges in the later part of the simulation, when the positive trend in the natural CO_2 flux exceeds the negative trend in the anthropogenic CO_2 flux (see also Figure 1f). This analysis suggests that, when observing trends in the Southern Ocean CO_2 sink, one must consider both the region being observed, and the multidecadal CO_2 flux variability within that region.

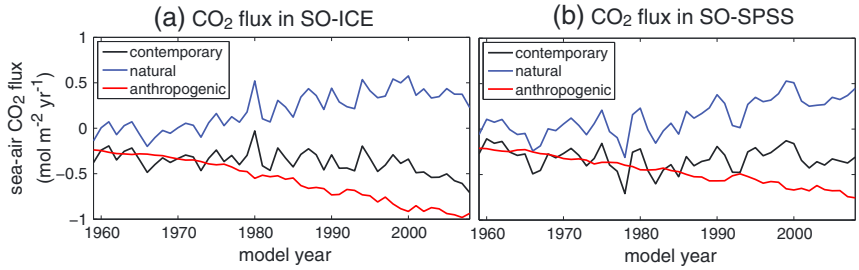

Figure 5. Average annual-mean fluxes of natural, anthropogenic, and contemporary CO_2 in the (a) SO-ICE and (b) SO-SPSS regions (mol C m^{-2} yr^{-1}).

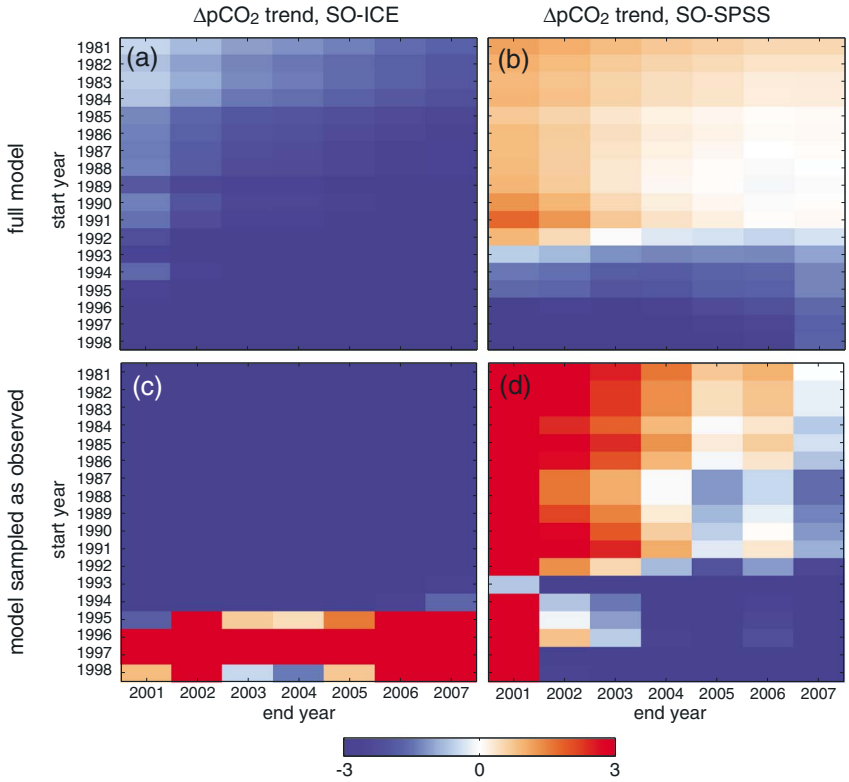

Figure 6. Trends in the average ΔpCO_2 for (first column) the SO-ICE region and (second column) the SO-SPSS region for the (first row) full model and (second row) model sampled as observed for a range of start and end years in the observed period. Units are μatm decade^{-1}, and red indicates times when ocean pCO_2 is rising faster than atmospheric pCO_2.

In the observed period, trends in ΔpCO_2 exhibit different behaviors in the two Southern Ocean biomes (Figure 6). In SO-ICE, the ΔpCO_2 trends are negative for all start and end year pairs, indicating that atmospheric pCO_2 is always rising faster than oceanic pCO_2 in this region of the model (Figure 6a). In our model, this region is characterized by significant vertical advection and mixing [see, e.g., *Lovenduski et al.*, 2013], so the negative ΔpCO_2 trend here is likely driven by an upwelling of water with low anthropogenic CO_2 content relative to the atmosphere. There is some gradation in the SO-ICE ΔpCO_2 trend plot (Figure 6a), hinting at interannual to decadal variability in this region. Nevertheless, we do not find a weakening of the Southern Ocean CO_2 sink in the SO-ICE region. This disagrees with *Fay et al.* [2014], who find significant positive trends in this region using available pCO_2 observations (see, e.g., Figure 3d of *Fay et al.* [2014]). In order to address the disagreement, we subsampled the monthly model output where pCO_2^{oc} observations have been collected, using the Lamont Doherty Earth Observatory surface ocean pCO_2 database described in *Fay et al.* [2014]. The subsampled model reveals positive ΔpCO_2 trends near the end of the timeseries that were not present in the full model result (cf. Figures 6a and 6c) and suggests that the observations, post-1995, are not able to recover the correct trends in this region. Further disagreement between model and observations may arise from model circulation biases in this region [*Danabasoglu et al.*, 2012].

In SO-SPSS, our model predicts positive ΔpCO_2 trends for many start and end year pairs in the observed period through the mid-1990s and negative ΔpCO_2 trends thereafter (Figure 6b). The subsampled model reveals similar ΔpCO_2 trends to the full model (cf. Figures 6b and 6d), suggesting that observational sampling in this biome is sufficient to reveal general decadal trend patterns. Modeled ΔpCO_2 trends are nearly identical to those seen in the observational record for the SO-SPSS biome (cf. Figure 6b, Figure 6d, and Figure 3c of *Fay et al.* [2014]; note their end year extends through 2010). While detection of the weakening Southern Ocean CO_2 sink in SO-SPSS may be possible in the early observed period, both model and observations suggest a strengthening of the CO_2 sink in this region since the mid 1990s. This switch from positive to negative trends in SO-SPSS signifies that, since the mid 1990s, atmospheric pCO_2 has been

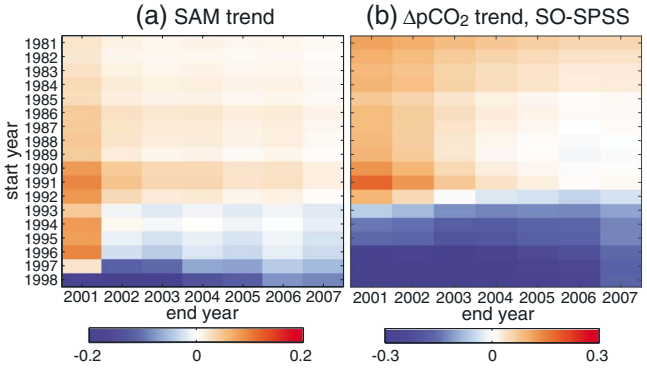

Figure 7. Trends in (a) the Southern Annular Mode (SAM) index (standard deviations per year) and (b) SO-SPSS average ΔpCO_2 (μatm yr^{-1}) for a range of start and end years in the observed period.

rising faster than oceanic pCO_2, perhaps in part due to the increase in anthropogenic CO_2 emissions (see also Figure 3).

Trends in ΔpCO_2 are affected by climate-driven variability on interannual to decadal timescales. Figure 7a depicts the trends in the model-derived Southern Annular Mode (SAM) index for a range of start and end years in the observed period. Positive trends in the SAM are synonymous with an increase in the surface westerly wind stress [*Thompson et al.*, 2000] and are known to drive enhanced upwelling of natural carbon and positive trends in pCO_2^{oc} in models [*Lovenduski et al.*, 2008]. In the early observed period, SAM exhibits a positive trend, but the positive SAM trend disappears and becomes negative in the later part of the observed period. This switch in the SAM trend, when combined with higher trends in pCO_2^{atm} at the end of the observed period, causes a strengthening of the Southern Ocean CO_2 sink in SO-SPSS (cf. Figures 7a and 7b).

The detection of multidecadal trends in ΔpCO_2 is affected by a number of factors, including the size of the trend to be detected, the spatial and temporal distribution of available data, and the magnitude of variance and autocorrelation in the data. As our model has perfect coverage in space and continuous coverage in time, the length of the time series needed to detect a trend is dependent only on the size of the trend to be detected, and the variance and autocorrelation in the monthly residuals after the trend has been removed. We use monthly model ΔpCO_2 output to investigate the length of the time series needed to detect a weakening of the CO_2 sink with 90% confidence, using the method of *Weatherhead et al.* [1998] (see equation (1)). At each location, we calculate the standard deviation (σ_N) and autocorrelation (ϕ) in de-trended ΔpCO_2 over the simulated period and solve for the detection time (n^*). We simplify our analysis by using a spatially uniform ω_o, noting that the estimate of the detection time is strongly influenced by the magnitude of the trend we are trying to detect, i.e. it takes longer to detect a smaller trend. Figure 8a shows the length of the time series in years required to detect a ΔpCO_2 trend of 8.4 μatm decade^{-1} at every location in the Southern Ocean (ω_o); this number corresponds to the ΔpCO_2 trend reported in *Takahashi et al.* [2012] (24.4 μatm decade^{-1} minus 16 μatm decade^{-1}). The required length of the time series for detection ranges from as low as 7 years at some mid-latitude locations to as high as 52 years at some high-latitude and coastal locations. The average time to detection in each biome is the average of all values of n^* in that biome. On average, 13 years of data are required to detect a weakening of this magnitude in SO-SPSS, and 17 years of data are required in SO-ICE, though there is large spatial heterogeneity in both

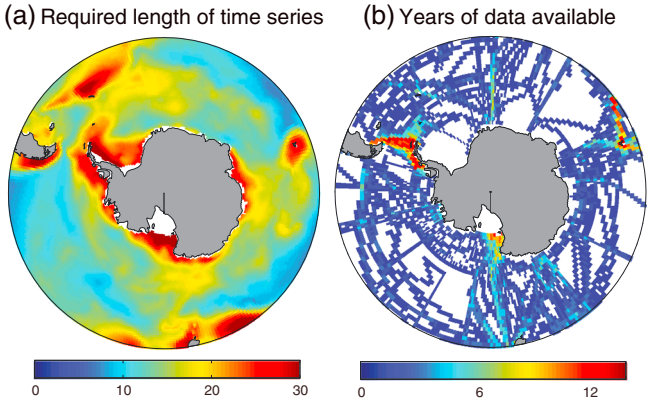

Figure 8. (a) Model-estimated length of ΔpCO_2 time series in years needed to detect a ΔpCO_2 trend of 8.4 μatm decade^{-1} with at least 90% confidence. (b) Number of years with at least 1 month of ΔpCO_2 data available.

biomes. This is in general agreement with *Majkut et al.* [2014] who find that 24 years of continuous monthly measurements are required to detect a reduction of Southern Ocean CO_2 uptake due to changes in climate. We conclude from this analysis that, with perfect data coverage in space and time, the weakening of the Southern Ocean CO_2 sink can be detected sooner in SO-SPSS than in SO-ICE.

In the real world, ΔpCO_2 trend detection is affected not only by variance and autocorrelation, but also by the spatial and temporal distribution of available data. Figure 8b depicts the number of years with at least one month of available pCO_2^{oc} data from 1981 to 2010, based on the data set described in *Fay and McKinley* [2013]. The number of years with at least one month of available data ranges from 0 to 13 years. We note that, in contrast to the model, the data are not continuously collected; some locations may have been occupied in only two years, but the length of the time series (i.e., the gap between occupations) may be several decades long. Frequent reoccupations of a particular location can provide insight into the local variance and autocorrelation that are central to detecting statistically robust trends. Our analysis suggests that the middle of Drake Passage is a promising place to detect such trends, as the pCO_2^{oc} data are nearly continuous and the required length of time series is small here.

4. Conclusions

We use output from a hindcast simulation (1958–2007) of an ocean biogeochemical and ecological model to address questions about the utility of surface ocean pCO_2 data in estimating multidecadal trends in the Southern Ocean CO_2 sink. We find that ΔpCO_2 trends can be used as a proxy for trends in contemporary air-sea CO_2 flux, as trends in piston velocity and solubility make only small contributions to the CO_2 flux trend. Positive trends in ΔpCO_2 indicate a weakening CO_2 sink, while negative trends indicate a strengthening sink. Observed trends must be interpreted with caution, as they are based on only slight differences between atmospheric and oceanic pCO_2 trends. The spatial pattern and magnitude of the CO_2 flux trends are sensitive to the period being analyzed; due to large interannual, decadal, and multidecadal variability, one must consider a range of start and end years before drawing conclusions about changes in the CO_2 sink. Wintertime CO_2 flux trends are indistinguishable from trends calculated using year-round data, suggesting that all available pCO_2^{oc} data be included in future analyses of the Southern Ocean CO_2 sink. In our model, a weakening of the CO_2 sink emerges from the SO-SPSS biome in the observed period, corresponding to times with positive trends in the SAM, but the weakening is not seen in the SO-ICE biome. Subsampling the model according to the observed pCO_2 record suggests that observational sampling in SO-SPSS is sufficient to reveal general decadal trend patterns, while in SO-ICE the observations, post-1995, are not able to recover the correct trends. Assuming perfect spatial and temporal coverage, we estimate that 13 years of data are required to detect a weakening of the CO_2 sink in SO-SPSS, while 17 years of data are required in SO-ICE. Given the imperfect data coverage and high variability in the Southern Ocean, it may not yet be possible to detect a weakening of the Southern Ocean CO_2 sink with much certainty. One feasible route to detection is to maintain the near continuous underway pCO_2 sampling in the Drake Passage that began in 2002 [*Sprintall et al.*, 2012].

Appendix A: Linear Taylor Expansion

In our model, the sea-air flux of CO_2, F is defined as follows:

$$F = (i - ifrac) \cdot pvel \cdot S \cdot \Delta pCO_2, \tag{A1}$$

where *ifrac* is the fraction of the ocean covered by sea ice, *pvel* is the piston velocity (also known as the gas transfer coefficient), S is the solubility of CO_2 in seawater, and ΔpCO_2 is the difference between the oceanic pCO_2 and the atmospheric pCO_2.

We investigate the contributions to the trend in the contemporary CO_2 flux, F' from trends in ΔpCO_2, piston velocity, solubility, and sea ice fraction using a linear Taylor expansion:

$$F' = \frac{\partial F}{\partial ifrac} ifrac' + \frac{\partial F}{\partial pvel} pvel' + \frac{\partial F}{\partial S} S' + \frac{\partial F}{\partial \Delta pCO_2} \Delta pCO_2', \tag{A2}$$

where the partial derivatives are calculated from model-estimated, regionally averaged quantities [see *Lovenduski et al.*, 2008, 2013].

Appendix B: pCO_2^{oc} Decomposition

We determine the mechanisms driving the trend in surface ocean pCO_2 by decomposing pCO_2 variability into two components: (1) the component driven by variability in surface temperature (pCO_2-T) and (2) the remaining variability due to biological and chemical factors (surface salinity, alkalinity, and DIC; pCO_2-nonT) according to *Takahashi et al.* [2002]:

$$pCO_2 - T = \overline{pCO_2} \times e^{0.0423(T_{obs} - \overline{T})}, and \tag{B1}$$

$$pCO_2 - nonT = pCO_{2,obs} \times e^{0.0423(\overline{T} - T_{obs})}, \tag{B2}$$

where $pCO_{2,obs}$ and T_{obs} represent the time-evolving pCO_2 and surface temperature averaged over a given region.

Acknowledgments
NSL is thankful for support from NSF (OCE-1155240) and NOAA (NA12OAR4310058). ARF and GAM are supported by NASA grants 07-NIP07-0036, NNX/11AF53G, and NNX/13AC53G. We are grateful to M. Long and K. Lindsay for providing access to model output (contact mclong@ucar.edu for data access). Computational facilities for the model simulations were provided by the Climate Simulation Laboratory, which is managed by CISL at NCAR. We thank C. Sweeney for helpful discussions.

References

Bretherton, C. S., M. Widmann, V. P. Dymnikov, J. M. Wallace, and I. Bladé (1999), The effective number of spatial degrees of freedom of a time-varying field, *J. Clim.*, *12*(7), 1990–2009.
Canadell, J. G., C. Le Quéré, M. R. Raupach, C. B. Field, E. T. Buitenhuis, P. Ciais, T. J. Conway, N. P. Gillett, R. A. Houghton, and G. Marland (2007), Contributions to accelerating atmospheric CO_2 growth from economic activity, carbon intensity, and efficiency of natural sinks, *Proc. Natl. Acad. Sci.*, *104*(47), 18,866–18,870, doi:10.1073/pnas.0702737104.
Danabasoglu, G., S. C. Bates, B. P. Briegleb, S. R. Jayne, M. Jochum, W. G. Large, S. Peacock, and S. G. Yeager (2012), The CCSM4 ocean component, *J. Clim.*, *25*(5), 1361–1389.
Doney, S. C., K. Lindsay, I. Fung, and J. John (2006), Natural variability in a stable, 1000-yr global coupled climate–carbon cycle simulation, *J. Clim.*, *19*(13), 3033–3054.
Fay, A. R., and G. A. McKinley (2013), Global trends in surface ocean pCO_2 from in situ data, *Global Biogeochem. Cycles*, *27*, 541–557, doi:10.1002/gbc.20051.
Fay, A. R., G. A. McKinley, and N. S. Lovenduski (2014), Southern Ocean carbon trends: Sensitivity to methods, *Geophys. Res. Lett.*, *41*, 6833–6840, doi:10.1002/2014GL061324.
Fox-Kemper, B., G. Danabasoglu, R. Ferrari, S. Griffies, R. Hallberg, M. Holland, M. Maltrud, S. Peacock, and B. Samuels (2011), Parameterization of mixed layer eddies. III: Implementation and impact in global ocean climate simulations, *Ocean Modell.*, *39*(1–2), 61–78.
Gent, P. R., and G. Danabasoglu (2011), Response to increasing southern hemisphere winds in CCSM4, *J. Clim.*, *24*(19), 4992–4998.
Gent, P. R., and J. C. McWilliams (1990), Isopycnal mixing in ocean circulation models, *J. Phys. Oceanogr.*, *20*(1), 150–155.
Griffies, S. M., et al. (2009), Coordinated Ocean-Ice Reference Experiments (COREs), *Ocean Modell.*, *26*(1–2), 1–46.
Henson, S. A., J. L. Sarmiento, J. P. Dunne, L. Bopp, I. Lima, S. C. Doney, J. John, and C. Beaulieu (2010), Detection of anthropogenic climate change in satellite records of ocean chlorophyll and productivity, *Biogeosciences*, *7*(2), 621–640, doi:10.5194/bg-7-621-2010.
Key, R. M., A. Kozyr, C. L. Sabine, K. Lee, R. Wanninkhof, J. L. Bullister, R. A. Feely, F. J. Millero, C. Mordy, and T. H. Peng (2004), A global ocean carbon climatology: Results from Global Data Analysis Project (GLODAP), *Global Biogeochem. Cycles*, *18*, GB4031, doi:10.1029/2004GB002247.
Khatiwala, S., F. Primeau, and T. Hall (2009), Reconstruction of the history of anthropogenic CO_2 concentrations in the ocean, *Nature*, *462*(7271), 346–349.
Large, W., and S. Yeager (2009), The global climatology of an interannually varying air–sea flux data set, *Clim. Dyn.*, *33*, 341–364.
Large, W. G., J. C. McWilliams, and S. C. Doney (1994), Oceanic vertical mixing: A review and a model with a nonlocal boundary layer parameterization, *Rev. Geophys.*, *32*(4), 363–403.
Le Quéré, C. (2010), Trends in the land and ocean carbon uptake, *Curr. Opin. Environ. Sustainability*, *2*(4), 219–224.
Le Quéré, C., et al. (2007), Saturation of the Southern Ocean CO_2 sink due to recent climate change, *Science*, *316*(5832), 1735–1738.
Le Quéré, C., T. Takahashi, E. T. Buitenhuis, C. Rödenbeck, and S. C. Sutherland (2010), Impact of climate change and variability on the global oceanic sink of CO_2, *Global Biogeochem. Cycles*, *24*, GB4007, doi:10.1029/2009GB003599.
Lenton, A., and R. J. Matear (2007), Role of the Southern Annular Mode (SAM) in Southern Ocean CO_2 uptake, *Global Biogeochem. Cycles*, *21*, GB2016, doi:10.1029/2006GB002714.
Lenton, A., N. Metzl, T. Takahashi, M. Kuchinke, R. J. Matear, T. Roy, S. C. Sutherland, C. Sweeney, and B. Tilbrook (2012), The observed evolution of oceanic pCO_2 and its drivers over the last two decades, *Global Biogeochem. Cycles*, *26*, GB2021, doi:10.1029/2011GB004095.
Lenton, A., et al. (2013), Sea–air CO_2 fluxes in the Southern Ocean for the period 1990–2009, *Biogeosciences*, *10*(6), 4037–4054, doi:10.5194/bg-10-4037-2013.
Long, M. C., K. Lindsay, S. Peacock, J. K. Moore, and S. C. Doney (2013), Twentieth-century oceanic carbon uptake and storage in CESM1(BGC), *J. Clim.*, *26*(18), 6775–6800, doi:10.1175/JCLI-D-12-00184.1.
Lovenduski, N. S., and T. Ito (2009), The future evolution of the Southern Ocean CO_2 sink, *J. Mar. Res.*, *67*(5), 597–617, doi:10.1357/002224009791218832.
Lovenduski, N. S., N. Gruber, S. C. Doney, and I. D. Lima (2007), Enhanced CO_2 outgassing in the Southern Ocean from a positive phase of the Southern Annular Mode, *Global Biogeochem. Cycles*, *21*, GB2026, doi:10.1029/2006GB002900.
Lovenduski, N. S., N. Gruber, and S. C. Doney (2008), Toward a mechanistic understanding of the decadal trends in the Southern Ocean carbon sink, *Global Biogeochem. Cycles*, *22*, GB3016, doi:10.1029/2007GB003139.
Lovenduski, N. S., M. C. Long, P. R. Gent, and K. Lindsay (2013), Multi-decadal trends in the advection and mixing of natural carbon in the Southern Ocean, *Geophys. Res. Lett.*, *40*, 139–142, doi:10.1029/2012GL054483.
Majkut, J. D., B. R. Carter, T. L. Frölicher, C. O. Dufour, K. B. Rodgers, and J. L. Sarmiento (2014), An observing system simulation for Southern Ocean carbon dioxide uptake, *Philos. Trans. R. Soc. London, Ser. A*, *372*(2019), 20130046, doi:10.1098/rsta.2013.0046.

McKinley, G. A., A. R. Fay, T. Takahashi, and N. Metzl (2011), Convergence of atmospheric and North Atlantic carbon dioxide trends on multidecadal timescales, *Nat. Geosci.*, *4*(9), 606–610.

Metzl, N. (2009), Decadal increase of oceanic carbon dioxide in Southern Indian Ocean surface waters (1991–2007), *Deep Sea Res. Part II*, *56*(8–10), 607–619, doi:10.1016/j.dsr2.2008.12.007.

Moore, J. K., and O. Braucher (2008), Sedimentary and mineral dust sources of dissolved iron to the world ocean, *Biogeosciences*, *5*(3), 631–656.

Moore, J. K., S. C. Doney, and K. Lindsay (2004), Upper ocean ecosystem dynamics and iron cycling in a global three-dimensional model, *Global Biogeochem. Cycles*, *18*, GB4028, doi:10.1029/2004GB002220.

Munro, D., N. Lovenduski, B. Stephens, T. Newberger, K. Arrigo, T. Takahashi, P. Quay, J. Sprintall, N. Freeman, and C. Sweeney (2015), Estimates of net community production in the Southern Ocean determined from time series observations (2002–2011) of nutrients, dissolved inorganic carbon, and surface ocean pCO_2 in Drake Passage, *Deep Sea Res., Part II*, doi:10.1016/j.dsr2.2014.12.014.

Santer, B. D., T. M. L. Wigley, J. S. Boyle, D. J. Gaffen, J. J. Hnilo, D. Nychka, D. E. Parker, and K. E. Taylor (2000), Statistical significance of trends and trend differences in layer-average atmospheric temperature time series, *J. Geophys. Res.*, *105*(D6), 7337–7356, doi:10.1029/1999JD901105.

Sarmiento, J. L., and C. Le Quéré (1996), Oceanic carbon dioxide uptake in a model of century-scale global warming, *Science*, *274*(5291), 1346–1350, doi:10.1126/science.274.5291.1346.

Sprintall, J., T. K. Chereskin, and C. Sweeney (2012), High-resolution underway upper ocean and surface atmospheric observations in Drake Passage: Synergistic measurements for climate science, *Oceanography*, *25*(3), 70–81.

Strutton, P. G., N. S. Lovenduski, M. Mongin, and R. Matear (2012), Quantification of Southern Ocean phytoplankton biomass and primary productivity via satellite observations and biogeochemical models, *CCAMLR Sci.*, *19*, 247–265.

Takahashi, T., et al. (2002), Global sea-air CO_2 flux based on climatological surface ocean pCO_2, and seasonal biological and temperature effects, *Deep Sea Res. Part II*, *49*(9–10), 1601–1622, doi:10.1016/S0967-0645(02)00003-6.

Takahashi, T., et al. (2009), Climatological mean and decadal change in surface ocean pCO_2, and net sea-air CO_2 flux over the global oceans, *Deep Sea Res. Part II*, *56*(8–10), 554–577, doi:10.1016/j.dsr2.2008.12.009.

Takahashi, T., C. Sweeney, B. Hales, D. W. Chipman, T. Newberger, J. G. Goddard, R. A. Iannuzzi, and S. C. Sutherland (2012), The changing carbon cycle in the Southern Ocean, *Oceanography*, *3*, 26–37.

Thompson, D. W. J., J. M. Wallace, and G. C. Hegerl (2000), Annular modes in the extratropical circulation. Part II: Trends, *J. Clim.*, *13*(5), 1018–1036.

Verdy, A., S. Dutkiewicz, M. J. Follows, J. Marshall, and A. Czaja (2007), Carbon dioxide and oxygen fluxes in the Southern Ocean: Mechanisms of interannual variability, *Global Biogeochem. Cycles*, *21*, GB2020, doi:10.1029/2006GB002916.

Wang, S., and J. K. Moore (2012), Variability of primary production and air-sea CO_2 flux in the Southern Ocean, *Global Biogeochem. Cycles*, *26*, GB1008, doi:10.1029/2010GB003981.

Waugh, D. W., F. Primeau, T. DeVries, and M. Holzer (2013), Recent changes in the ventilation of the Southern Oceans, *Science*, *339*(6119), 568–570, doi:10.1126/science.1225411.

Weatherhead, E. C., et al. (1998), Factors affecting the detection of trends: Statistical considerations and applications to environmental data, *J. Geophys. Res.*, *103*(D14), 17,149–17,161, doi:10.1029/98JD00995.

Wetzel, P., A. Winguth, and E. Maier-Reimer (2005), Sea-to-air CO_2 flux from 1948 to 2003: A model study, *Global Biogeochem. Cycles*, *19*, GB2005, doi:10.1029/2004GB002339.